

## Surface-relaxation-induced giant corrugation on graphite (0001)

Shigeki Kawai<sup>1,2,\*</sup> and Hideki Kawakatsu<sup>1</sup>

<sup>1</sup>*Institute of Industrial Science, The University of Tokyo and CREST,*

*Japan Science and Technology Agency, Komaba 4-6-1, Meguro-ku, Tokyo 153-8505, Japan*

<sup>2</sup>*Department of Physics, University of Basel, Klingelbergstr. 82, Basel 4056, Switzerland*

(Received 15 January 2009; published 30 March 2009)

Soft graphite surface was atomically resolved by ultrasmall amplitude dynamic force microscopy operating at 5 MHz. The giant corrugation amplitude of up to 85 pm appeared due to local vertical deformations of the graphite surface. In simultaneous scanning tunneling microscopy and dynamic force microscopy, all of the symmetric C atoms were resolved with the conservative interaction in the repulsive regime. Additionally, the dissipative interaction showed a large difference of asymmetric  $\alpha$  and  $\beta$  site C atoms, arising from the different mechanical properties. The low stiffness of the graphite surface played a crucial role in the observations at room temperature.

DOI: [10.1103/PhysRevB.79.115440](https://doi.org/10.1103/PhysRevB.79.115440)

PACS number(s): 68.37.Ps, 34.20.Cf, 62.25.-g, 81.05.Uw

The graphite surface has been one of the most extensively studied surfaces with scanning probe microscopy. The surface with the hexagonal lattice has two different kind of sites, namely, the  $\alpha$  and the  $\beta$  site C atoms. The  $\alpha$  site atoms are directly above in the adjacent planes, whereas the  $\beta$  site atoms are located above the hollow sites. In general, the  $\beta$  site atoms are only visible with scanning tunneling microscopy (STM).<sup>1,2</sup> Observation of all atoms has been challenging due to the asymmetry of the electric and mechanical properties. Observed corrugation amplitudes are usually varied and were up to several angstrom,<sup>3,4</sup> commonly known as the “giant corrugations.” It is inconsistent to values of around 20 pm obtained by the first-principles calculation and the He scattering measurement.<sup>5,6</sup> It has been assumed that deformations of the graphite surface layer by interaction forces between the STM tip and the sample increase the observed corrugation amplitude.<sup>7</sup> Graphite has a laminated structure, and the surface layer is connected to the second layer with weak interactions, arising from the overlap of partially occupied  $p_z$  orbitals perpendicular to the three hybridized orbitals [van der Waals (vdW) force type]. On the other hand, in the plane, C atoms are strongly connected to each other by  $sp^2$  covalent bonds. This strong difference results in the high compliance in the laminated direction. Although this assumption is widely accepted, the giant corrugation has been observed only with STM, which traces the surface with a given charge density.

Dynamic force microscopy (DFM) is another well-known technique to resolve surfaces with atomic resolution.<sup>8</sup> Since the tip-sample distance is usually regulated at a negative slope of the time-averaged interaction force gradient via a negative frequency shift of a cantilever,<sup>9</sup> all kind of surfaces, such as insulators, semiconductors, and metals, can be observed.<sup>10</sup> In the case of semiconductor surfaces, the strong interaction of the covalent bonding enables discriminations of surface atoms even in the same IV group.<sup>11</sup> On the other hand, vdW surfaces, such as graphite, carbon nanotubes, and C60, are one of the most challenging surfaces even for atomically resolved imaging due to their extremely low reactivity and small C-C distance of 142 pm. These features act to reduce the corrugation amplitude in DFM. Moreover since the stiffness of the interlayer between the first and sec-

ond layers is very low, a stable imaging at a closer tip-sample distance to enhance the interactions is difficult while avoiding deformations. Atomically resolved observations have been hence demonstrated only at low temperature (LT),<sup>12–15</sup> where the minimum detectable interaction force can be made at least 2 orders of magnitude smaller than at room temperature (RT). Observations with atomic resolution at RT has remained a great challenge. This surface is suitable for studying the phenomena in the observation of soft sample in DFM.

Here, we demonstrate atomically resolved imaging on the graphite surface with small amplitude DFM at RT. The giant corrugation was observed at a constant frequency shift mode. At a closer tip-sample distance controlled with a tunneling current feedback, atomic features with the sixfold and threefold symmetries were observed by conservative and dissipative interactions, respectively.

All experiments were performed with our homemade ultrahigh vacuum (UHV) DFM, operating at RT.<sup>16</sup> The clean graphite (0001) surface was obtained by cleaving with a polyimide adhesive tape in the preparation chamber ( $P < 2 \times 10^{-7}$  Pa). In order to detect small variation in interaction between tip and sample, the following two techniques were applied. First, an ultrasharp tip (nanosensor: SSS-NCH) with a nominal radius of 2 nm was carefully prepared to reduce the background long-range vdW force. Native SiO<sub>2</sub> layers on the tip were etched by vapor HF just before introducing into the UHV chamber, and then H atoms presumably terminating the Si tip were removed by gentle Ar<sup>+</sup> sputtering ( $t = 30$  min,  $P_{\text{Ar}} = 1.3 \times 10^{-4}$  Pa,  $I_{\text{ion}} < 0.1 \mu\text{A}$ , and  $U_{\text{ex}} = 610$  eV). Second, higher flexural resonance modes of the cantilever were used. Higher modes have higher effective stiffness, and hence a stable ultrasmall amplitude operation for selective detections of the short-range interaction can be implemented.<sup>17,18</sup> High resonance frequencies ( $> 1$  MHz) of the modes are also expected to enhance the detection sensitivity.<sup>9</sup> Thermal drifts in the images were corrected afterward, and the measurements were analyzed with the WSXM program.<sup>19</sup>

Figure 1(a) shows the DFM topography of the graphite surface obtained with the second resonance mode. The constant frequency shift  $\Delta f_{2\text{nd}}$  and the amplitude  $A_{2\text{nd}}$  were

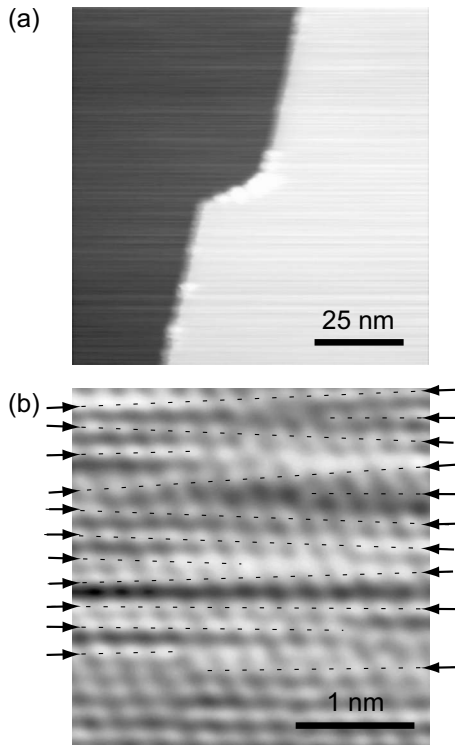


FIG. 1. DFM topographies of the graphite surface obtained with the second resonance mode. (a)  $100 \times 100 \text{ nm}^2$ ,  $f_{2\text{nd}} = 1.765\,551 \text{ MHz}$ ,  $Q_{2\text{nd}} = 8211$ ,  $A_{2\text{nd}} = 650 \text{ pm}$ ,  $\Delta f_{2\text{nd}} = -30 \text{ Hz}$ , and the applied bias voltage  $V_{\text{bias}} = 0 \text{ V}$ . (b)  $3 \times 3 \text{ nm}^2$ ,  $f_{2\text{nd}} = 1.737\,255 \text{ MHz}$ ,  $Q_{2\text{nd}} = 8156$ ,  $A_{2\text{nd}} = 220 \text{ pm}$ ,  $\Delta f_{2\text{nd}} = -28 \text{ Hz}$ , and  $V_{\text{bias}} = 0.2 \text{ V}$ .

$-30 \text{ Hz}$  and  $650 \text{ pm}$ , respectively. A clear monoatomic step was observed. The step height of approximately  $320 \text{ pm}$  was very close to the interlayer distance of  $335 \text{ pm}$ . Figure 1(b) shows the atomically resolved DFM topography in an area of  $3 \times 3 \text{ nm}^2$ . In order to enhance the detection sensitivity of short-range interaction, the amplitude was reduced to  $220 \text{ pm}$ , and then the frequency shift was adjusted to  $-28 \text{ Hz}$ . Observed corrugation amplitude of less than  $10 \text{ pm}$  was nearly equal to one of  $12 \text{ pm}$  measured at LT.<sup>20</sup> A previous theoretical calculation shows that the hollow site should be observed as the maxima in the attractive regime due to the summation of the six C-Si interactions, and the  $\alpha$  site should be observed as the second protrusion.<sup>20</sup> Therefore, the observed maxima in Fig. 1(b) should be the hollow site, and the resolution was not sufficient to resolve the  $\alpha$  site. Some disordered features, which are indicated by arrows, were also confirmed. It is most likely that deformations in either the graphite surface layer or the tip should be the reason for the distortions of the image. The interlayers of graphite are much softer than the Si tip, and deformations of a local part of graphite surface layer must be dominant. Since the tip-sample distance was regulated with a constant negative frequency shift, the attractive interaction force may have pulled up the first layer toward the tip.

Figure 2 shows DFM topographies obtained with the third resonance mode. The third resonance mode has a higher stiffness than the second resonance mode, and a more stable oscillation can be expected at small amplitudes. The slow

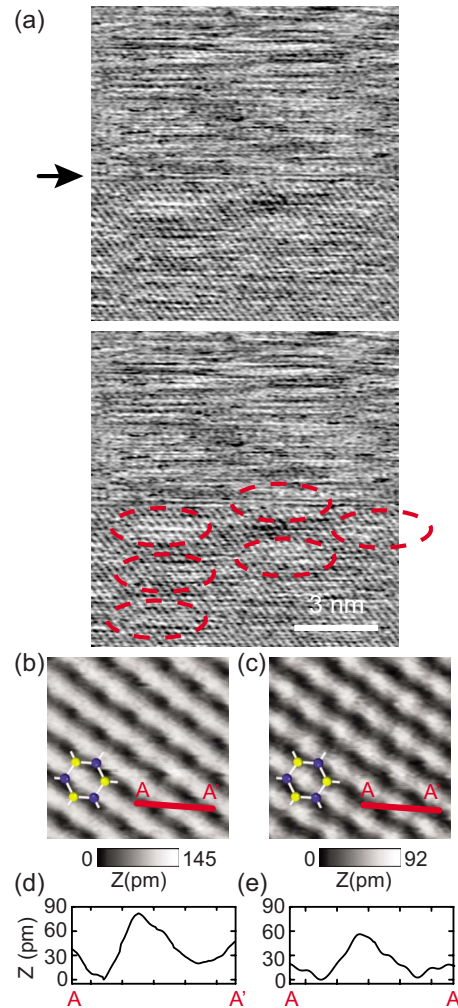


FIG. 2. (Color online) DFM topographies obtained with the third resonance mode. (a)  $\Delta f_{3\text{rd}} = -13 \text{ Hz}$ ,  $A_{3\text{rd}} = 120 \text{ pm}$ ,  $V_{\text{bias}} = 0.2 \text{ V}$ , and  $11 \times 11 \text{ nm}^2$ . (b)  $f_{3\text{rd}} = -6 \text{ Hz}$ . (c)  $f_{3\text{rd}} = +52 \text{ Hz}$ . [(d) and (e)] Line profiles along  $A-A'$  in (b) and (c), respectively.  $A_{3\text{rd}} = 210 \text{ pm}$ ,  $V_{\text{bias}} = 0 \text{ V}$ , and  $1.2 \times 1.2 \text{ nm}^2$ . The  $\alpha$  site (yellow). The  $\beta$  site (blue).  $f_{3\text{rd}} = 4.790\,437 \text{ MHz}$  and  $Q_{3\text{rd}} = 10\,085$ .

scan direction was from top to bottom. At the middle of the image, the corrugation amplitude suddenly increased as indicated with an arrow in Fig. 2(a). No significant jump of the topographic height signal, relating to tip deformations, was observed. A weak feature with a long periodicity of  $3 \text{ nm}$  indicated by red circles in the same image, which looks like the giant lattice structure observed in STM,<sup>21</sup> was also visible. Figure 2(b) shows the DFM topography obtained with  $A_{3\text{rd}} = 210 \text{ pm}$  at  $\Delta f_{3\text{rd}} = -6.0 \text{ Hz}$  in an area of  $1.2 \times 1.2 \text{ nm}^2$ . A clear atomic contrast was observed. Beside the hollow site, the  $\alpha$  site atoms were also detected. The inset shows a schematic drawing of the hexagonal C atom ring. Although the imaging contrast was similar to those in the previous results, the corrugation amplitude was surprisingly large ( $\approx 85 \text{ pm}$ ) as shown in Fig. 2(d), and was seven times larger than the theoretical value.<sup>20</sup> So far, the giant corrugation has been widely observed in STM, but it has never been seen by DFM. As observed in Fig. 1(b), deformations of the first layer play an important role to enhance the corrugation

amplitude. In contact mode AFM, repulsive interaction forces have been shown to elastically deform the several layers from the graphite surface. Calculations indicated that the sublayers make the first layer harder, and deformations of the first layer hence becomes smaller by increasing the counting number of layers.<sup>22</sup> On the other hand, in the case of attractive interaction forces, pulling forces act mainly on the first graphite layer. Therefore, the stiffness of the first layer must have a strong asymmetry in the  $Z$  direction, and its deformation by pulling must be larger. Consequently, the small variation in interaction on the vdW surface would be enhanced by tip-induced deformations of the first layer, and the giant corrugation was observed. This situation is completely opposite to that in measurements of the ionic crystal surfaces.<sup>23,24</sup> In that case, the Si tip is usually terminated with the sample material and hence becomes very soft. The stiffness of the tip should be much lower than that of the surface due to its low coordinate. When the interaction between tip and sample is caused, the tip dominantly deforms and the corrugation amplitude is hence enhanced.

With the same polarity of the  $Z$  feedback, the frequency shift could be reduced (more positive) while keeping the atomic resolution. Surprisingly, it could reach a positive value. Figure 2(c) shows the DFM topography at  $\Delta f_{3rd} = +52$  Hz. The small corrugation of the  $\alpha$  site atom disappeared, and a small change in the corrugation amplitude was also confirmed as shown in Fig. 2(e). When the tip was fully retracted from the surface, the resonance frequency regained to the initial value. Therefore, the positive frequency shift was not due to the thermal drift of the resonance frequency but due to the tip-sample interaction. The jump-to-contact instability is caused in the case that

$$k_0 < \frac{\partial}{\partial Z_0} \frac{1}{2\pi} \int_0^{2\pi} F[Z_0 + A_{3rd}(1 + \cos \theta)] d\theta, \quad (1)$$

where  $Z_0$  is the closest distance in the oscillation. However, this situation cannot exist with a static spring constant  $k_0$  of approximately 42 N/m,  $A_{3rd} = 210$  pm, and an ultra-sharp tip under the small vdW interaction force  $F$  of much less than 1 nN.<sup>25</sup> Moreover, if the tip were macroscopically connected to the surface by the instability, the contact resonance frequency should have been shifted at least in the order of several kHz. A more reasonable possibility is that the first graphite layer is elastically deformed by interactions and moved toward the tip apex. In this case, the tip-surface potential has several minima due to the movement of the first graphite layer, and the positive slope of the frequency shift could be caused even in a positive frequency shift region. The amplitude was so small that the tip could stay at a certain negative slope of the interaction force gradient, and a stable imaging could be realized. The event shown by the arrow in Fig. 2(a) is presumably the sign of the jump from the first negative slope to the second one. Since this feature was not observed with the LT measurements,<sup>12-15</sup> the large thermal energy at RT would have assisted to switch to the second negative slope of interaction force gradient. A similar interaction potential curve with several minima has been observed on a highly flexible molecule (see Fig. 2 in Ref. 26). Presumably,

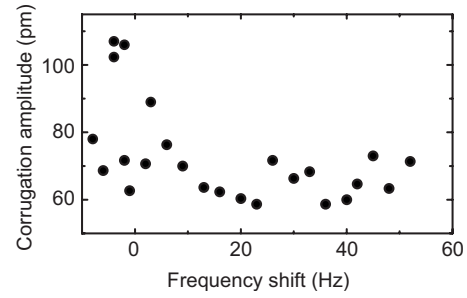


FIG. 3. Observed corrugation amplitude as a function of the frequency shift.

the mechanism to produce the modulated potential is essentially the same. However, in this experiment, the amplitude of 210 pm was so small that the mobile first layer would accompany the tip motion in the oscillation. Otherwise, the large dissipative interaction, arising from the hysteresis loop of the interaction force,<sup>27</sup> should have prevented stable imaging. Figure 3 shows the summary of the corrugation amplitude in the images obtained at 24 different frequency shifts with the same amplitude of 210 pm. Each corrugation amplitude was calculated by averaging over three line profiles along with same direction  $A-A'$ . No clear tendency was confirmed. It seems that once the first graphite layer was in contact with the tip, the frequency shift in the range did not play a role in the corrugation amplitude so much. The key factor to produce the large corrugation should be whether the first layer is in contact with the tip or not. This assumption is in good agreement to the situation in STM. The giant corrugation is haphazard and is nearly uncontrollable.

The low stiffness of the surface layer also played a crucial role in observation in the repulsive regime. Figure 4 shows the simultaneously detected conservative and dissipative interactions and the STM topographic images obtained with

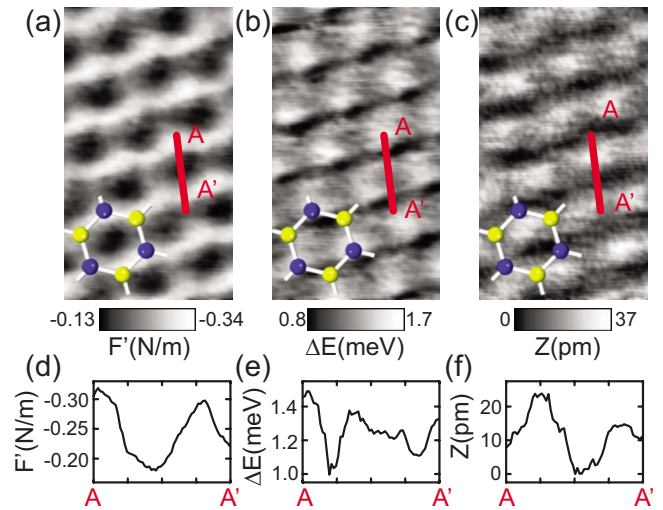


FIG. 4. (Color online) (a) Conservative and (b) dissipative interaction maps and (c) STM topography. [(d)–(f)] Line profiles along  $A-A'$  in (a), (b), and (c), respectively. Image size:  $0.71 \times 1.2$  nm<sup>2</sup>,  $V_{\text{bias}} = -0.8$  V, and  $\bar{I}_t = 400$  pA. The cantilever was the same as in Fig. 1(b).  $A'_{2nd} = 50$  pm. The  $\alpha$  site (yellow). The  $\beta$  site (blue).



the second resonance mode. The tip-sample distance was regulated with a time-averaged tunneling current  $\bar{I}_t$  of 400 pA at  $V_{\text{bias}} = -0.8$  V. The fast scan direction was from left to right. The cantilever was oscillated with the constant excitation mode.<sup>28</sup> The amplitude far from the surface  $A'_{2\text{nd}}$  was 50 pm, and the averaged damped amplitude at the surface was approximately 23 pm. At the tunneling distance, a positive frequency shift was detected on the entire surface. Due to the low stiffness of the interlayer, the slope of the repulsive interaction is gradual.<sup>29</sup> In other words, the amplitude of around 23 pm was small enough to realize a direct force gradient measurement. Therefore, conservative and dissipative interactions can be simply converted as

$$F' = -\frac{k_{2\text{nd}}\Delta f_{2\text{nd}}}{2f_{2\text{nd}}}, \quad (2)$$

$$\Delta E = \frac{k_{2\text{nd}}(A'^2_{2\text{nd}} - A^2_{2\text{nd}})}{2Q_{2\text{nd}}}. \quad (3)$$

An effective stiffness  $k_{2\text{nd}}$  of the second mode was simply set to 2000 N/m for the calculations. As shown in Fig. 4(a), all of C atoms were observed in the conservative interaction map. Contrary, a threefold symmetric feature was detected by dissipative interactions as shown in Fig. 4(b). In DFM, the dissipative interaction is mainly caused by the hysteresis loop of the interaction force between forward and backward in one oscillation,<sup>27</sup> and stabilities of sample and tip are usually the key factors. The  $\beta$  site atoms are positioned above the hollow site of the second layer and so that these stiffness should be lower than those of the  $\alpha$  site atoms. Therefore, the observed corrugation in Fig. 4(b) should be the  $\beta$  site atom. The amount of detected dissipative interaction was found to be at least 1 order of magnitude smaller than that in the previous LT measurement with  $A = 250$  pm.<sup>29</sup> It is presumably due to the smaller hysteresis loop of the interaction force.<sup>30</sup> When the amplitude is smaller than the hysteresis loop, the amount of the dissipative interaction becomes smaller. In other words, ultrasmall amplitude DFM disables the criterion of small amplitude operation proposed by Giessibl.<sup>31</sup> Especially on surfaces of the soft samples, this feature gives a stable imaging condition. Distortions of the observed corrugation was similar to the stick slip feature in

lateral force microscopy (LFM).<sup>32</sup> In this experiment, the amplitude was so small that the tip was always connected to the graphite surface in the whole one oscillation cycle. Therefore, a shear force could be caused. The lateral stiffness of the cantilever and its tip are higher than the binding stiffness of the graphite interlayer, and a lateral shift of the first layer should be caused by the interactions. It is likely that the surface C atom or a local part of the first layer followed the tip scan movement, and when the lateral force exceeded a certain threshold, the C atom jumped back to its initial position. This feature is in good agreement with previous theoretical studies.<sup>33</sup> Figure 4(c) shows the simultaneously recorded STM topography. With the imaging parameters, the maximum tunneling current should flow at the  $\beta$  site,<sup>1,2</sup> but the maxima were shifted from the  $\beta$  sites. In the case of the graphite surface, the tip mainly traces a constant local density of state (LDOS) at the Fermi energy of the surface, and the LDOS might be modulated by tip-sample interactions. If this assumption “modulated LDOS” is correct, the mechanism of the giant corrugation in STM can be explained with our DFM results. On the hollow site, the first layer is lifted up with the attractive interaction force as shown in Figs. 2(b) and 2(c) and is observed as maxima. On the other hand, the surface C atoms are pushed down to the second layer with the repulsive force as shown in Fig. 4. In this experiment, no strong giant corrugation in STM topography ( $\sim 23$  pm) was observed, but the oscillating tip presumably relaxed deformations of the first graphite layer.

In this work, we demonstrate high-resolution imaging by small amplitude DFM with higher modes of a sharp Si cantilever. Enhanced sensitivity enabled the atomically resolved imaging of the soft graphite surface even at RT. The giant corrugation amplitude was observed in the second positive slope of the frequency shift. With this experimental results obtained by DFM, it can be concluded that the mechanical interaction produces the giant corrugation. All of C atoms were resolved by the conservative interaction. On the other hand, only the  $\beta$  site was resolved by the dissipative interaction.

The author (S.K.) would like to thank Alexis Baratoff and Thilo Glatzel for many helpful discussions. This work was financially supported by JST-CREST.

\*shigeki.kawai@unibas.ch

<sup>1</sup>D. Tománek, S. G. Louie, H. J. Mamin, D. W. Abraham, R. E. Thomson, E. Ganz, and J. Clarke, *Phys. Rev. B* **35**, 7790 (1987).

<sup>2</sup>D. Tománek and S. G. Louie, *Phys. Rev. B* **37**, 8327 (1988).

<sup>3</sup>G. Binnig, H. Fuchs, C. Gerber, H. Rohrer, E. Stoll, and E. Tosatti, *Europhys. Lett.* **1**, 31 (1986).

<sup>4</sup>S.-I. Park and C. F. Quate, *Appl. Phys. Lett.* **48**, 112 (1986).

<sup>5</sup>A. Selloni, P. Carnevali, E. Tosatti, and C. D. Chen, *Phys. Rev. B* **31**, 2602 (1985).

<sup>6</sup>W. E. Carlos and M. W. Cole, *Surf. Sci.* **91**, 339 (1980).

<sup>7</sup>J. M. Soler, A. M. Baro, N. Garcia, and H. Rohrer, *Phys. Rev.*

*Lett.* **57**, 444 (1986).

<sup>8</sup>F. J. Giessibl, *Science* **267**, 68 (1995).

<sup>9</sup>T. R. Albrecht, P. Grütter, D. Horne, and D. Rugar, *J. Appl. Phys.* **69**, 668 (1991).

<sup>10</sup>S. Morita, R. Wiesendanger, and E. Meyer, *Noncontact Atomic Force Microscopy* (Springer, Berlin, 2002).

<sup>11</sup>Y. Sugimoto, P. Pou, M. Abe, P. Jelinek, R. Pérez, S. Morita, and O. Custance, *Nature (London)* **446**, 64 (2007).

<sup>12</sup>W. Allers, A. Schwarz, U. D. Schwarz, and R. Wiesendanger, *Appl. Surf. Sci.* **140**, 247 (1999).

<sup>13</sup>A. Schwarz, U. D. Schwarz, S. Langkat, H. Hölscher, W. Allers,

- and R. Wiesendanger, *Appl. Surf. Sci.* **188**, 245 (2002).
- <sup>14</sup>M. Ashino, A. Schwarz, T. Behnke, and R. Wiesendanger, *Phys. Rev. Lett.* **93**, 136101 (2004).
- <sup>15</sup>S. Hembacher, F. J. Giessibl, J. Mannhart, and C. F. Quate, *Proc. Natl. Acad. Sci. U.S.A.* **100**, 12539 (2003).
- <sup>16</sup>S. Kawai, D. Kobayashi, S. Kitamura, S. Meguro, and H. Kawakatsu, *Rev. Sci. Instrum.* **76**, 083703 (2005).
- <sup>17</sup>S. Kawai, S. Kitamura, D. Kobayashi, S. Meguro, and H. Kawakatsu, *Appl. Phys. Lett.* **86**, 193107 (2005).
- <sup>18</sup>S. Kawai and H. Kawakatsu, *Appl. Phys. Lett.* **88**, 133103 (2006).
- <sup>19</sup>I. Horcas, R. Fernandez, J. Gomez-Rodriguez, J. Colchero, J. Gomez-Herrero, and A. Baro, *Rev. Sci. Instrum.* **78**, 013705 (2007).
- <sup>20</sup>H. Hölscher, W. Allers, U. D. Schwarz, A. Schwarz, and R. Wiesendanger, *Phys. Rev. B* **62**, 6967 (2000).
- <sup>21</sup>J. Xhie, K. Sattler, M. Ge, and N. Venkateswaran, *Phys. Rev. B* **47**, 15835 (1993).
- <sup>22</sup>N. Sasaki and M. Tsukada, *Phys. Rev. B* **52**, 8471 (1995).
- <sup>23</sup>C. Barth, A. S. Foster, M. Reichling, and A. L. Shluger, *J. Phys.: Condens. Matter* **13**, 2061 (2001).
- <sup>24</sup>W. A. Hofer, A. S. Foster, and A. L. Shluger, *Rev. Mod. Phys.* **75**, 1287 (2003).
- <sup>25</sup>M. Ashino, A. Schwarz, H. Hölscher, U. D. Schwarz, and R. Wiesendanger, *Nanotechnology* **16**, S134 (2005).
- <sup>26</sup>C. Loppacher, M. Guggisberg, O. Pfeiffer, E. Meyer, M. Bamberlin, R. Lüthi, R. Schlittler, J. K. Gimzewski, H. Tang, and C. Joachim, *Phys. Rev. Lett.* **90**, 066107 (2003).
- <sup>27</sup>N. Sasaki and M. Tsukada, *Jpn. J. Appl. Phys.* **39**, L1334 (2000).
- <sup>28</sup>A. Schirmeisen, H. Hölscher, B. Anczykowski, D. Weiner, M. M. Schäfer, and H. Fuchs, *Nanotechnology* **16**, S13 (2005).
- <sup>29</sup>S. Hembacher, F. J. Giessibl, J. Mannhart, and C. F. Quate, *Phys. Rev. Lett.* **94**, 056101 (2005).
- <sup>30</sup>P. M. Hoffmann, S. Jeffery, J. B. Pethica, H. Özgür Özer, and A. Oral, *Phys. Rev. Lett.* **87**, 265502 (2001).
- <sup>31</sup>F. J. Giessibl, *Rev. Mod. Phys.* **75**, 949 (2003).
- <sup>32</sup>C. M. Mate, G. M. McClelland, R. Erlandsson, and S. Chiang, *Phys. Rev. Lett.* **59**, 1942 (1987).
- <sup>33</sup>M. Harada, M. Tsukada, and N. Sasaki, *e-J. Surf. Sci. Nanotechnol.* **5**, 126 (2007).